

PPPL-5266

Multi-energy x-ray detector calibration for T_e and impurity density (n_z) measurements of MCF plasmas

J. Maddox, N. Pablant, A. S. Kruer, S. E. LaPointe, K. W. Hill, M. Bitter, M.L. Reinke, T. A. M. T. Donath, B. Luethi, B. Stratton

August 2016



Prepared for the U.S. Department of Energy under Contract DE-AC02-09CH11466.

Princeton Plasma Physics Laboratory

Report Disclaimers

Full Legal Disclaimer

This report was prepared as an account of work sponsored by an agency of the United States Government. Neither the United States Government nor any agency thereof, nor any of their employees, nor any of their contractors, subcontractors or their employees, makes any warranty, express or implied, or assumes any legal liability or responsibility for the accuracy, completeness, or any third party's use or the results of such use of any information, apparatus, product, or process disclosed, or represents that its use would not infringe privately owned rights. Reference herein to any specific commercial product, process, or service by trade name, trademark, manufacturer, or otherwise, does not necessarily constitute or imply its endorsement, recommendation, or favoring by the United States Government or any agency thereof or its contractors or subcontractors. The views and opinions of authors expressed herein do not necessarily state or reflect those of the United States Government or any agency thereof.

Trademark Disclaimer

Reference herein to any specific commercial product, process, or service by trade name, trademark, manufacturer, or otherwise, does not necessarily constitute or imply its endorsement, recommendation, or favoring by the United States Government or any agency thereof or its contractors or subcontractors.

PPPL Report Availability

Princeton Plasma Physics Laboratory:

<http://www.pppl.gov/techreports.cfm>

Office of Scientific and Technical Information (OSTI):

<http://www.osti.gov/scitech/>

Related Links:

[U.S. Department of Energy](#)

[U.S. Department of Energy Office of Science](#)

[U.S. Department of Energy Office of Fusion Energy Sciences](#)

Multi-energy x-ray detector calibration for T_e and impurity density (n_Z) measurements of MCF plasmas^{a)}

J. Maddox¹, N. Pablant¹, P. Efthimion¹, L. Delgado-Aparicio¹, K.W. Hill¹, M. Bitter¹, M.L. Reinke², M. Rissi³, T. Donath³, B. Luethi³, B. Stratton¹

¹PPPL, 100 Stellarator Rd, Princeton, NJ 08540, USA

²Oak Ridge National Laboratory, 1 Bethel Valley Rd, Oak Ridge, TN 37831, USA

³DECTRIS Ltd., Taefernweg 1, 5405 Baden-Daettwil, Switzerland

(Dated: 22 June 2016)

Soft x-ray detection with the new "multi-energy" PILATUS3 detector systems holds promise as a magnetically confined fusion (MCF) plasma diagnostic for ITER and beyond. The measured x-ray brightness can be used to determine impurity concentrations, electron temperatures, $n_e^2 Z_{eff}$ products, and to probe the electron energy distribution. However, in order to be effective, these detectors which are really large arrays of detectors with photon energy gating capabilities must be precisely calibrated for each pixel. The energy-dependence of the detector response of the multi-energy PILATUS3 system with 100K pixels has been measured at Dectris Laboratory. X-rays emitted a tube under high voltage bombards various elements such that they emit x-ray lines from Zr-L α to Sn-K α between 1.8 and 22.16 keV. Each pixel on the PILATUS3 can be set to a minimum energy threshold in the range from 1.6 to 25 keV. This feature allows a single detector to be sensitive to a variety of x-ray energies, so that it is possible to sample the energy distribution of the x-ray continuum and line-emission. PILATUS3 can be configured for 1D or 2D imaging MCF plasmas with typical spatial, energy, and temporal resolution of 1 cm, 0.6 keV, and 5 ms, respectively.

I. MOTIVATION AND BACKGROUND

Flexible, non perturbing diagnostics are necessary for control, stability, and understanding of any high temperature plasma such as magnetically or inertially confined fusion plasmas¹. Multi-energy x-ray profiles can diagnose plasma electron temperatures². In addition, the results in this paper indicate that by measuring x-ray emissions of different energies a multi-energy x-ray system can also measure impurity concentrations by measuring the perturbing effect of bound-bound characteristic line emissions on the continuum background. The diagnosis of temperature and impurity density are correlated however, but with sufficient information of x-ray emissions from different energies both the concentration and temperature can be solved simultaneously.

With these promising results in mind this paper discusses the calibration and energy dependent characteristics of a water-cooled PILATUS3 100k x-ray detector produced by Dectris Ltd. The detector has an array of 195x487 photodiode pixels which are capable of measuring photon counts up to $10^7/s$, without any saturation effects, at 2 ms intervals. Each 147 square micron pixel detects a count when a photon of sufficient energy is absorbed by 450 microns of n-doped Si³. Upon absorption the photon generates electron charge cloud and the number of electrons in the cloud depends on the energy of the photon. The charge cloud will trigger a count for

that pixel if it is sufficient to surpass the internal voltage bias of the pixel, which is set by the user of the detector. This voltage bias is set through 3 separate voltage settings, V_{cmp} sets the minimum threshold on all of the pixels across the detector. V_{trm} is the value in which the pixel-wise energy thresholds are incremented through a 6 bit DAC which allows 64 different energy threshold settings for for each pixel, and V_{rf} which sets the detector wide gain on the photon generated electron cloud. If we consider a simple detector configuration with rows of repeating groups of energy thresholds and a pinhole camera like that used in²; the large number of independent energy discriminating pixels allow for a profile of lines of sight and in addition to many different energy gate levels allowing the ratio of photons of different energies to be analyzed across the plasma.

The goals of the calibration include measuring detector response for three unique energy ranges 2-8 keV, 3-12 keV, and 6-24 keV, while using as many of the 64 trimbits as possible to in those energy ranges to the maximize energy resolution in that range. In addition, it is necessary to characterize the energy dependent detector responses to eliminate systematic errors in the ratios between x-ray emissions of different energy. These factors include the widths of the energy thresholds and an additional response when the energy of the photon is less than the energy of the threshold. This procedure must be performed for each pixel because their response varies across the detector.

^{a)}Contributed paper published as part of the Proceedings of the 21st Topical Conference on High-Temperature Plasma Diagnostics, Madison, Wisconsin, June, 2016.

II. METHOD OF CALIBRATION AND ENERGY RANGES

This calibration seeks to characterise the PILATUS3 for energy ranges which can be used to discriminate between different impurities commonly present in MCF plasma which have characteristic line emissions in the chosen energy range^{7,8}. With this mind, the 2-8 keV range is desirable because of the strong Mo and Ar line-emissions at those energies in addition to some access to Fe, Cu, and W lines. In addition because photon emission rates are most often proportional to the exponential of the ratio of the photon energy and the plasma temperature - the lowest energy range extends the lower temperature limit of the diagnostic and extends the reach its to cooler regions of the plasma. On the other end, the 6-24 keV range has higher energy Mo lines which are completely isolated from Ar lines so that a Mo concentration could be more accurately determined. In addition identifying the higher energy Mo lines allows for better analysis of non-thermal electron tails during LHCD and ECRH but is limited to only the hottest plasmas to generate sufficient signal to noise. The 3-12 keV range strikes a balance between the two and also has improved access to Fe, Cu, and W emissions but is more limited in discriminating Mo and Ar.

The first step of the calibration is to measure the detector response across trimbit values for different characteristic line emissions of different energy. The calibration response curves are generated from 14 element bombarded from a x-ray tube under high voltage to generate characteristic lines which are used to calibrate PILATUS3 for the three unique energy ranges. The normalized detector response curves are shown in figure 1 and the fit used are shown in equations 1-4. The response curves indicate how characteristic lines are ‘seen’ on the PILATUS3. Because only 64 energy threshold settings are possible with the PILATUS system increasing the range of the energy thresholds decreases the energy resolution of the thresholds.

$$S_{Det} = S_{line} + S_{oth} + S_{background} \quad (1)$$

The function used to fit the detector response is broken down into three parts S_{line} the part associated with the characteristic line emission being used in the calibration,

$$S_{line} = [I_{line} + a_{lineShr}(x_{trm} - Trm_{line})] \text{erfc}\left(\frac{x_{trm} - Trm_{line}}{\sqrt{2}Trm_{width_{line}}}\right)/2, \quad (2)$$

and a companion high energy line S_{oth} is fit with another error function complement ($\text{erfc} = [1 - \text{erf}]$) this extra response curve could also be associated with the element emitting a higher energy tail of diffuse emissions,

$$S_{oth} = I_{oth} \text{erfc}\left(\frac{x_{trm} - Trm_{oth}}{\sqrt{2}Trm_{width_{oth}}}\right), \quad (3)$$

also included in the fit are background emissions which are higher energy than the max energy threshold of the settings

considered,

$$Background = b_{background} + a_{backShr}(x_{trm} - Trm_{line}). \quad (4)$$

This calibration focuses on the parameters used to fit the detectors response to the characteristic line emission S_{line} . The inflection point, Trm_{line} in equation 2, of each line emission’s response curve establishes the non-linear relation between trimbit and energy. It is shown that when the line intensity is at 50% then the energy threshold is set to the energy of the characteristic line⁷. The width of the detector’s response to the line is related to $(Trm_{width_{line}})$. Also $(a_{lineShr})$ relates to the rate of response of the detector due to charge sharing between pixels. An understanding of these energy dependent effects and their relative importance is required to reliably solve for impurity densities from line cluster ratios and T_e from the slope of the background continuum.

III. PIXEL-WISE ENERGY RESOLUTION AND CHARGE SHARING

Previous papers on the characterization of the PILATUS2 gives some intuition to the energy widths and charge sharing effects of the of the PILATUS3^{5,6}. However, a detailed analysis is necessary to account the for energy dependence of these effects to be a reliable impurity diagnostic The future use of the PILATUS3 as a plasma diagnostic requires a functional energy dependent relation that can be included in the analysis of plasma emissivities for each energy range setting.

The $Trm_{width_{line}}$ fit parameter in equation 2 is related to the full width of each detector response curve in trimbit, black curves in figure 2. To translate this width to energy we multiply this parameter with the energy per trimbit (blue) or each of the trimbit widths at their respective trimbit values (averaging to yield the energy/trimbit for the inflection point, Trm_{line}). This translation into energy space from trimbit space (black*blue = red) is plotted for each energy range in figure 2. This width constrains counts of photons with energy less than the energy threshold at each energy threshold and its deviation from a heaviside response. Also shown in the blue curve in 2 is how variation from non-linearity between trimbit and energy depends on detector settings.

The detector also exhibits a linear response from photons of energy larger or close to that of the threshold settings of the pixel. This effect is attributed in Kraft and Pablant to primarily originating from charge sharing between pixels leading to double or missing counts when a photon of sufficient energy strikes the area between pixels. In this case depending on the threshold settings and the energy of the photon the charge cloud could trigger a count on both or neither pixel when only one count should be recorded. This effect has been modelled as a function of the ratio between the area of the pixel and the area between pixels on the PILATUS2⁶. This paper seeks to understand the photon energy dependence of this linear term so that it can be accounted for in the analysis of diagnostic data. Here the $a_{lineShr}$ fit parameter in equation 2 indicates the additional response of the detector per trimbit away from the inflection point of the line. This translates into energy by multiplying this parameter with the trimbit per photon energy for each characteristic line, this process is displayed in figure 3.

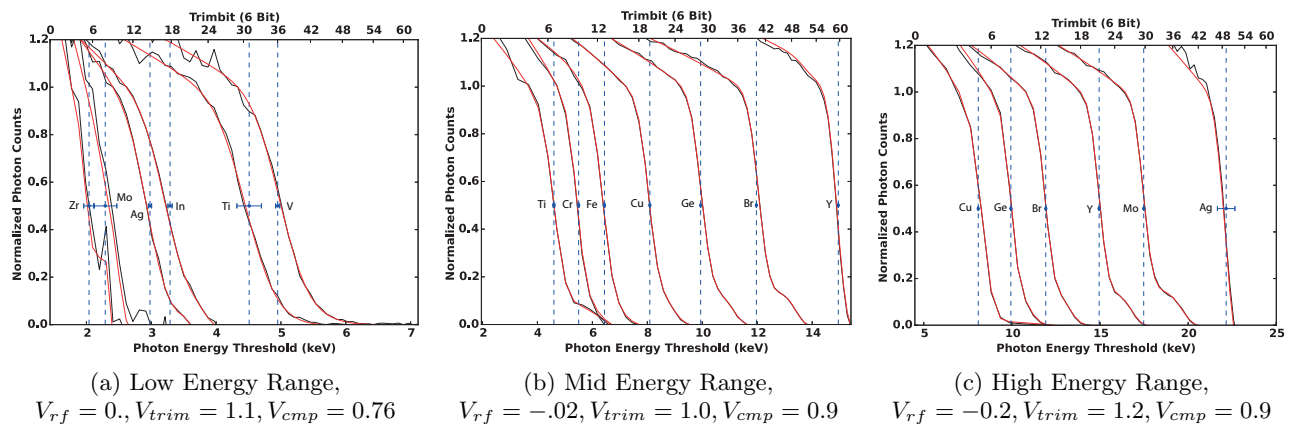


FIG. 1: S-Curves of Detector Response (Color Online)

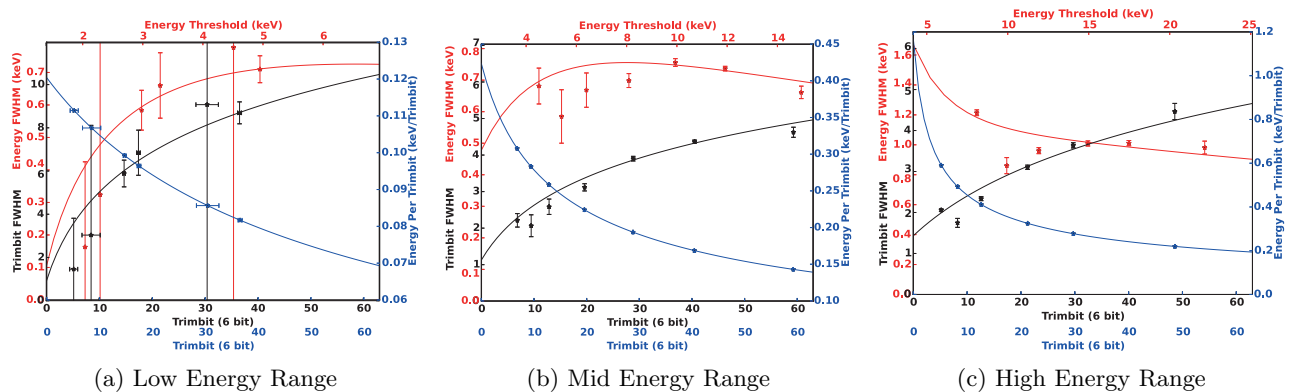


FIG. 2: Response Widths (Color Online)

IV. CONCLUSIONS AND FUTURE WORK

The calibrations and their parameters here will be used to diagnose Ar, Mo, and W concentration profiles for the final Alcator C-Mod campaign. In addition to being able to map energy thresholds to trimbit, the energy dependent features of the detector are accounted for. Calibrating the energy width of the PILATUS3 response and modelling the energy dependence of the additional response are essential to using a broad energy range to diagnose impurities. Functional curves of these parameters are generated from a characteristic line emission calibration at Dectris Ltd. For future use of the low energy threshold settings it is important to remove attenuation from the air perhaps by pumping He into the region between the detector and the pinhole. Also in the high energy range the absorption of Si drops off and if this region proves to be interesting the CdTe detectors have 100% in this range⁹.

ACKNOWLEDGEMENTS

This work was performed at Dectris Ltd. and with support from US DOE Contract No. DE-AC02-09CH11466 at PPPL and support from DE-AC02-09CH11466.

- ¹L. Delgado-Aparicio, et al. DOE/Office of Science Program Office: Office of Fusion Energy Sciences (2014).
- ²J. Maddox *et al* submitted Nucl. Fusion
- ³Pilatus Detection Systems User Manual. Version 1.3 Dectris. (2011).
- ⁴N. A. Pablant, L. Delgado-Aparicio, *et al.*, Rev. Sci. Instrum. **83**, 10E526 (2012).
- ⁵P. Kraft, *et al.*, IEEE TRANSACTIONS ON NUCLEAR SCIENCE, VOL. **56**, NO. 3, JUNE 2009 .
- ⁶P. Kraft, *et al.*, J. Synchrotron Rad. (2009). **16**, 368?375 .
- ⁷M.L. Reinke, , *et al.*, Rev. Sci. Instrum., **83**, 113504, (2012).
- ⁸J. E. Rice, *et al.*, Phys. Rev. A, **53**, 3953, 1996.
- ⁹L. Delgado-Aparicio, *et al.*, PPPL Report Energy-resolved x-ray imaging for magnetically confined fusion plasmas: measurement of impurity concentration and thermal and non- Maxwellian electron distributions, Report 4977, <http://bp.pppl.gov/pubreport/2014/PPPL-4977.pdf>, (2014).

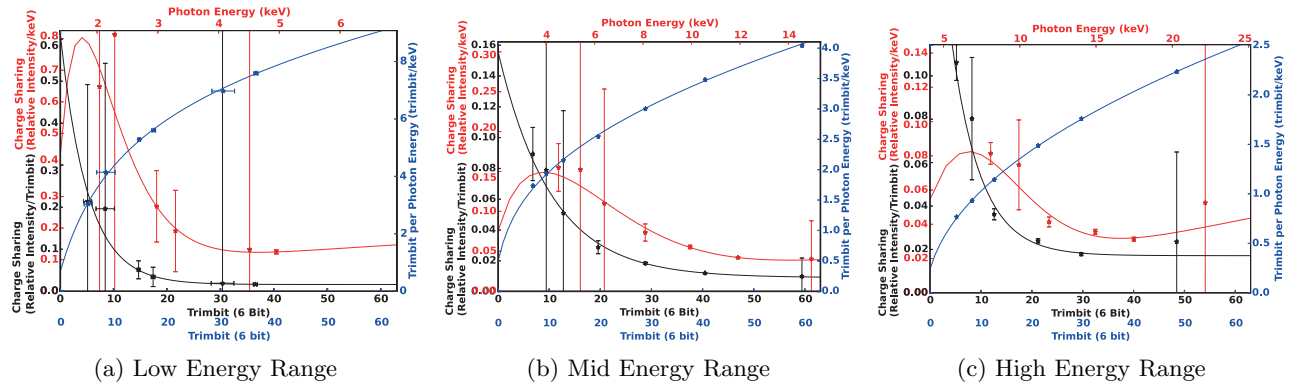


FIG. 3: Charge Sharing (Color Online)

Princeton Plasma Physics Laboratory Office of Reports and Publications

Managed by
Princeton University

under contract with the
U.S. Department of Energy
(DE-AC02-09CH11466)

P.O. Box 451, Princeton, NJ 08543
Phone: 609-243-2245
Fax: 609-243-2751

E-mail: publications@pppl.gov

Website: <http://www.pppl.gov>